

Extended-cavity grating-tuned operation of mid-infrared InAsSb diode lasers

M. Mürtz*, J.S. Wells, L. Hollberg, T. Zibrova, N. Mackie

Time and Frequency Division, National Institute of Standards and Technology, 325 Broadway, Boulder CO 80303, USA

Received: 8 July 1997/Revised version: 31 July 1997

Abstract. Novel InAsSb diode lasers have been operated in an extended-cavity grating-tuned configuration. These devices operate near liquid-nitrogen temperature and emit laser light in the spectral region near $\lambda = 3 \mu\text{m}$. We have developed a LN_2 cryostat that permits placement of both the collimation optics and the extended-cavity elements within a vacuum chamber. We have observed tuning of the laser frequency over a 1.44 THz (48 cm^{-1}) range by rotation of the external grating. This result was obtained without anti-reflection coating of the laser output facet.

PACS: 42.55.Px; 07.57.Hm

The mid-infrared (MIR) spectral region near $3 \mu\text{m}$ is very attractive for various spectroscopic applications, such as environmental monitoring and industrial process control, since many important molecules have strong vibrational absorption bands around this wavelength. Recently, InAsSb diode lasers have been developed and investigated for their suitability for trace gas monitoring [1, 2]. These novel III–V semiconductor lasers provide radiation in the spectral region near $3 \mu\text{m}$. This region can also be covered by IV–VI compound (lead salt) lasers. However, III–V diodes promise higher single-mode output power. CW single-mode optical power up to 10 mW has been demonstrated for an InAsSb injection laser at temperatures between 80 K and 110 K [3].

Among various approaches to tunable MIR laser sources (such as nonlinear conversion devices or sideband molecular gas lasers) that are currently being investigated by researchers, semiconductor lasers are advantageous because of their compactness and efficiency. In order to improve their tunability and spectral linewidth, it is desirable to operate the laser in an external cavity. One possible solution is the extended-cavity grating-tuned (ECGT) configuration. It has been widely used for line narrowing and frequency tuning

of room-temperature III–V semiconductor lasers that operate in the near-infrared (NIR) or visible region of the spectrum [4, 5]. Recently, broad tunability of optically pumped MIR III–V lasers has been demonstrated in an ECGT configuration [6], although research and development on III–V injection lasers are still in their early stages. These devices use a simple structure for electron and photon confinement and often show multi-mode emission. Moreover, operation of these devices is seriously complicated by the facts that they require a vacuum environment and that the beam is not visually discernible, even with the aid of a display card.

Few experiments on external-cavity MIR diode lasers have been carried out to date [7, 8]. Nevertheless, experiments at the University of Bonn, Germany, have led to a frequency-stabilized lead-salt laser with a 200 kHz linewidth and application to sub-Doppler molecular spectroscopy [9]. A major drawback of this system, however, is the restricted continuous tuning range. The successful experiments in Bonn have motivated us to work on further improvements for mid-infrared diode lasers.

In this paper we present our results on external grating tuning that have been achieved with the LN_2 -cooled InAsSb injection lasers described in [10]. We additionally describe the features of our ECGT system, which is based on an evacuated cryostat chamber that houses the laser and the optics for the extended cavity.

1 Experimental setup

The lasers used were double heterostructure (DH) diodes grown by liquid-phase epitaxy (LPE). They were designed to operate in the temperature range 80–120 K with a wavelength near $3.4 \mu\text{m}$, or a frequency of approximately 90 THz (3000 cm^{-1}). Quasi-single-mode operation was achievable at certain combinations of temperature and current. The laser chips were mounted in a standard housing for MIR diode lasers, which allowed access to only one of the two output beams. In the present investigation, two diode lasers were available. Threshold currents for these lasers were near 50 mA (laser 1) and 25 mA (laser 2).

* Author to whom correspondence should be addressed.

Present address: Institut für Angewandte Physik der Universität Bonn, Wegelerstr. 8, D-53115 Bonn, Germany
(Fax: +49-228/733 474, E-mail: muertz@uni-bonn.de)

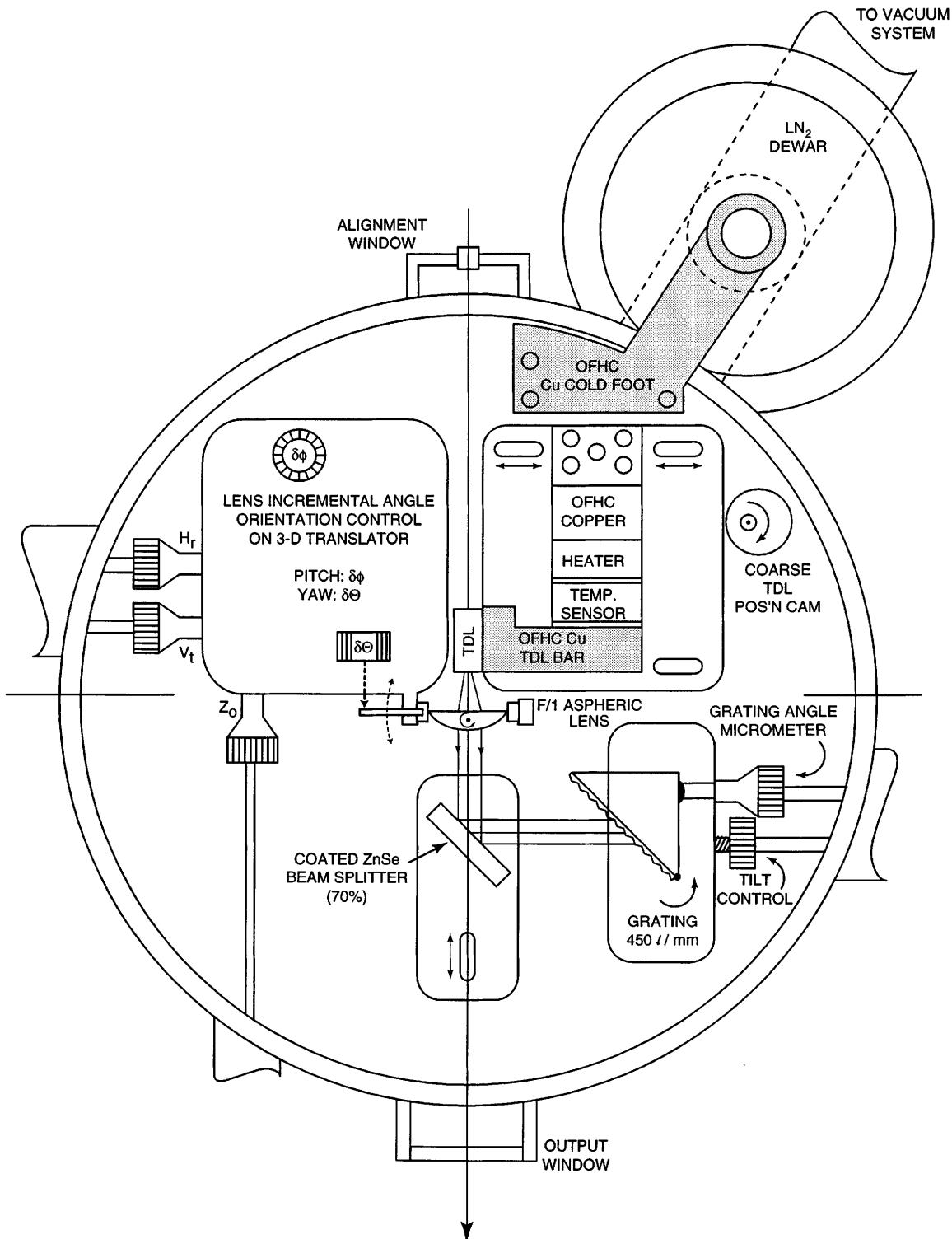


Fig. 1. Top view of the cryostat for the mid-infrared ECGT diode laser (schematically). The liquid-nitrogen reservoir is located in the upper part of the drawing. The diode laser sits in about the center of the vacuum chamber on a cold mounting platform. The collimation optics and external cavity elements are located within the chamber and can be controlled from outside

Our diode-laser system was designed for ECGT operation; the cavity was formed by one facet of the diode and an external reflecting diffraction grating as the tunable wavelength filter. Figure 1 shows a schematic diagram of the vacuum chamber that housed the laser and the external cavity elements. The chamber consisted of a stainless steel cylin-

der (outer diameter 32 cm, height 12 cm) covered by a 3 cm thick glass lid. A cold foot made of oxygen-free, high-conductivity (OFHC) copper was attached to the OFHC copper portion of the liquid-nitrogen Dewar tail. One end of an assembly consisting of several thin OFHC copper strips was clamped to the cold foot; the other end was clamped to the

OFHC copper bar/TDL-mounting platform (bar/platform). The bar/platform was supported by a temperature-isolating post on the support frame, and the mounting platform had a servo-controlled heater for temperature control. The holding time for the 1.5 liter liquid-nitrogen reservoir was about six hours, and the temperature achieved (depending on the number of heat-conducting strips) was generally in the 80 K range.

Collimation of the diode laser beam was achieved by means of an $f/1$, 25.4 mm focal-length lens which had compensation for spherical aberration. The lens was made of ZnSe and was anti-reflection (AR)-coated for $3.4\ \mu\text{m}$. It was supported by a high-precision, 3D translation stage that could be controlled by two-section rods consisting of a flexible rod to the stage and a solid rod fed through an o-ring seal to outside the chamber. The collimation optics were the most critical component of the external cavity. The coupling efficiency between the laser and the external cavity not only depended on the attenuation of the collimator but also on the wavefront distortion: a peak-to-peak wavefront distortion of $\lambda/4$ results in approximately 2 dB of reduction in coupling efficiency [11]. In the early stages of the experiment, we tested an off-axis parabola as well as some common lenses for collimation; however, none of these permitted sufficient coupling efficiency and we achieved only very low feedback levels.

A ZnSe beam splitter (BS) designed for a 45° angle of incidence was used for coupling a portion of the laser output to the external grating. The BS was coated on one side for 70% p-wave reflectance and AR-coated on the other side. The grating was a 450 line/mm echelette, with a nominal reflectance of 98% in the Littrow configuration. The distance between the laser chip and the grating was about 12 cm. Grating angle and tilt were also able to be controlled from outside the chamber by means of feed-throughs. Additionally, the grating could be scanned through one free spectral range (FSR) by means of a PZT ($8\ \mu\text{m}$ extension) between the micrometer and the grating-mount contact point. The cryostat was originally designed and developed for operation of lead-salt diode lasers in the ECGT configuration; further details of the cryostat-based system may be found elsewhere [12].

Optimal external-cavity performance requires a minimum residual reflectance of the laser output facet and a maximum coupling of the return beam from the grating back to the diode cavity. This means that the diode facet had to be AR coated. However, coating procedures for the MIR wavelength region above $2.5\ \mu\text{m}$ are more sophisticated than that for the visible or NIR because of coating material limitations. A further major difficulty came from the requirement that the coating had to withstand temperature cycling [12]. Our attempt to put an AR coating on laser 1 failed. Hence the following experiments have been performed with laser 2 (with the lower threshold current), which was not AR-coated.

2 Experimental results

An important condition for external-cavity operation is a correct alignment of laser and external optical elements. This alignment was very laborious to achieve in our experiments, since the infrared beam was not visible and the external cavity elements were not easily accessible when the chamber was evacuated. During our earlier efforts, we developed an align-

ment procedure for use with the chamber [12]. The laser chip, lens, and the grating were aligned in a multi-step procedure that used a red HeNe laser to serve as the pilot laser. The most critical alignment parameter was the distance between the aspheric lens and the laser chip. This distance had to be adjusted so that the beam waist at the diode laser facet was transformed into a nearly collimated beam incident on the grating.

Since this could not be done with the use of the pilot laser, we simplified the alignment procedure in a first step: the grating/BS setup was replaced by a partly transmitting reflector (nominal reflectance 80%) placed outside the chamber at normal incidence to the infrared beam. The distance between the reflector and laser facet was about 25 cm. The optimal lens position was then found by monitoring the effect of the optical feedback on the laser threshold current. For this purpose, a triangular current modulation was applied to the diode laser and the output beam was directed to an InAs photodiode. By that means, optical power vs. laser current could be displayed on an oscilloscope for a P-I plot. At optimum alignment, the feedback resulted in a significant decrease in threshold current as the photon loss of the external-cavity laser became less than that for the solitary laser. It was determined experimentally that the range of significant feedback for the lens position was about 3×10^{-4} times the lens focal length. Once the initial effect was found, the reflector orientation and the two 3D mount controls orthogonal to the focus control were able to be used to maximize the feedback. Figure 2 shows the resulting P-I plot with and without feedback. The threshold current has been decreased by about 20%.

In the next stage of the experiment, we returned to the operational setup where the in-chamber diffraction grating was being used as the external reflector. Once again, we observed a significant decrease in the threshold current as we tuned the grating angle such that it matched the diode laser frequency. Here the decrease in threshold was about 13% lower than the

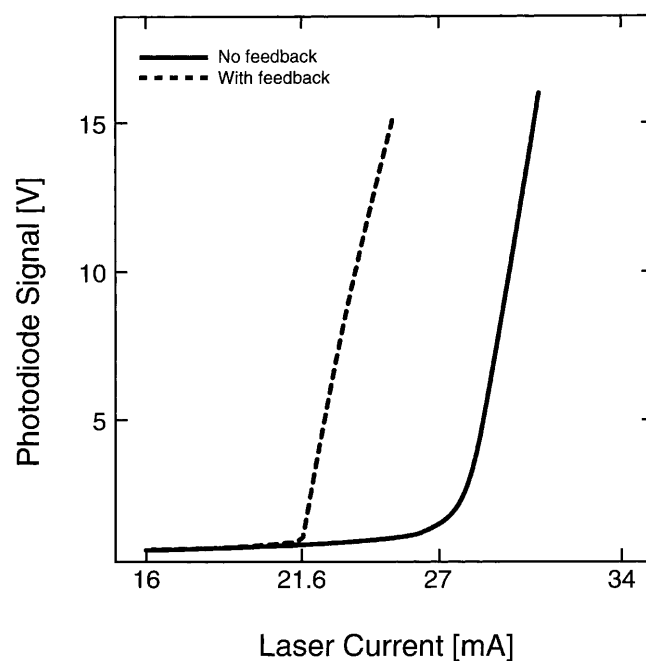


Fig. 2. Power vs. current plots of diode laser 2 without (solid line) and with (dashed line) optical feedback from an external 80% reflector

80% reflection, which was due to lower reflectance of the grating/BS combination (as, from the nominal 98% grating reflectance and twice the 70% at 45° from the BS, we can calculate a maximum reflectivity of less than 50%). In contrast, the feedback in these circumstances was more stable, since in the latter configuration the grating was sitting on the same base as the laser (not so for the case of the reflector outside the chamber). In addition there was reduced coupling of acoustic waves into the vacuum chamber. For a demonstration of the stability, the cavity parameters were adjusted such that a kink appeared in the P-I plot (see Fig. 3). This is interpreted as mode jump between two external-cavity modes. The feedback conditions were sufficiently stable to observe and record the curve, with the kink in the same position for over one minute.

An important question in this investigation was whether or not the diode laser could be tuned with the external grating. To analyze the spectral mode behavior, the diode laser beam was put through a monochromator with 3 GHz (0.1 cm^{-1}) resolution. Figure 4 shows three different recordings of emission spectra with the diode laser current near 1.6 times the threshold current. The laser current and temperature were fixed at the same value for all scans. The upper scan (a) was taken from the free-running diode laser without any external feedback. This spectrum shows a dominant mode near 91.74 THz (3060 cm^{-1}) and several other longitudinal modes with power considerably less than 10% of the dominant mode. The middle and bottom scans (b and c) are two examples of spectra of the laser with optical feedback from the grating. The spectra show a dominant ECGT laser mode and the solitary laser mode that is partially suppressed.

The wavelength of the dominant grating-tuned laser mode depends, as expected, on the grating angle (Fig. 5). By tun-

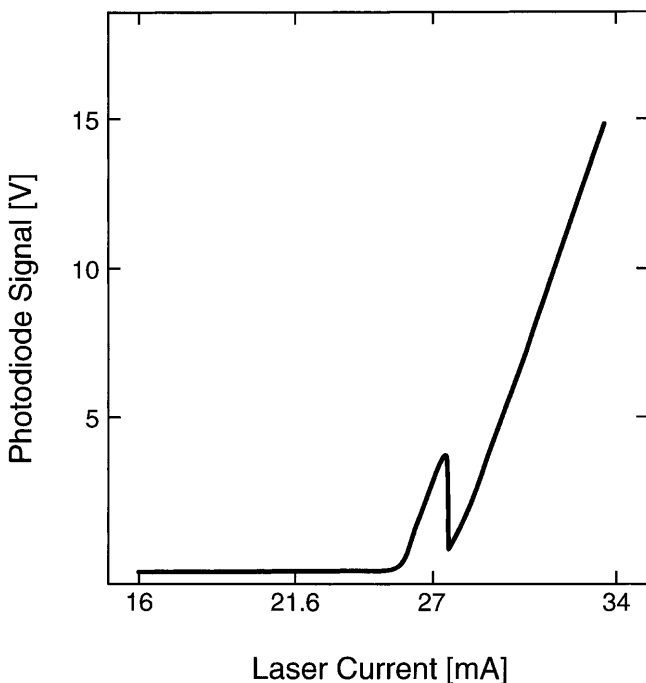


Fig. 3. Power vs. current plot of diode laser 2 in the ECGT configuration. The kink in the curve is interpreted as a mode jump between two external-cavity modes

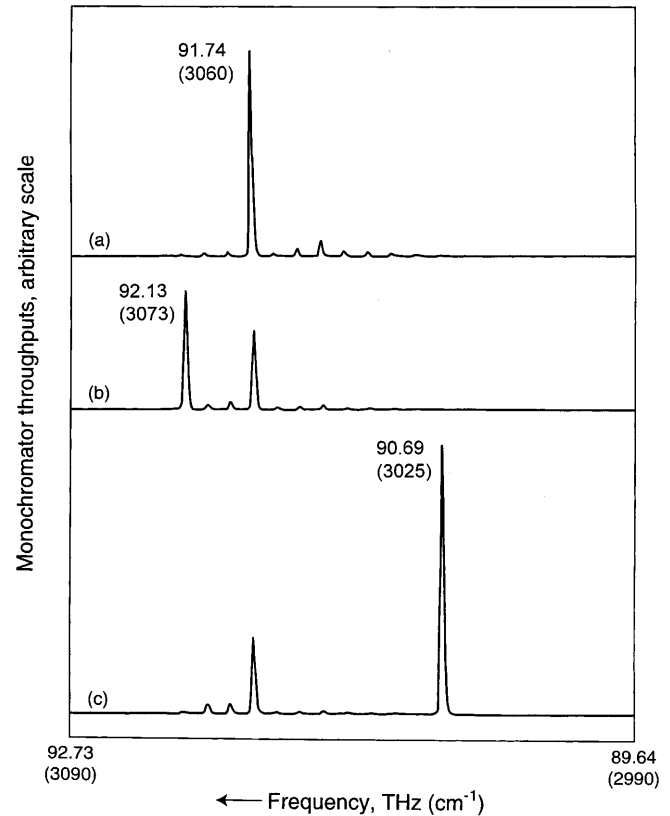


Fig. 4a-c. Lasing spectra from the ECGT laser taken **a** without feedback, and **b, c** with feedback from grating at different angles. Laser temperature and current were fixed at the same value for all spectra

ing the grating angle, we could bring the ECGT diode to lase at every frequency that matched the longitudinal-mode frequencies of the solitary diode. In each such case, the solitary laser mode was partially suppressed. The largest tuning achieved by rotating the grating was about 1.44 THz, shifting

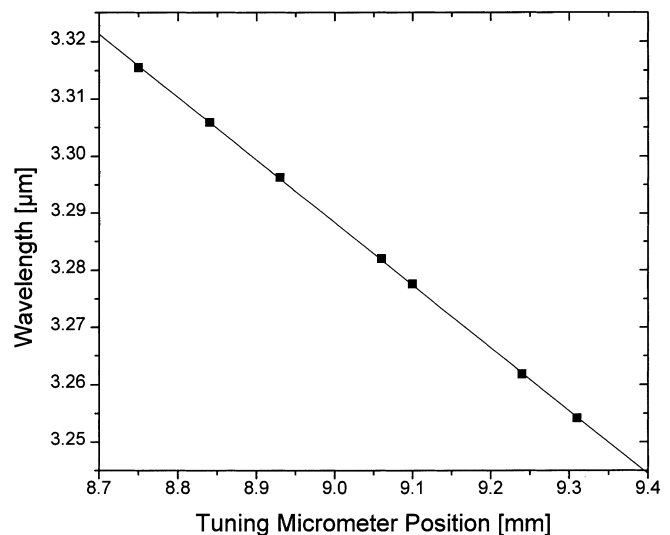


Fig. 5. Wavelength of dominant ECGT laser mode vs. position of the grating-tuning micrometer. Square symbols represent some (not all) grating-tuned laser modes. The micrometer tuning range corresponds to a grating angle range of about 1.2° centered near 47.7°

the frequency from 90.69 THz to 92.13 THz (48 cm^{-1} , from 3025 cm^{-1} to 3073 cm^{-1}). This frequency tuning clearly showed that the external cavity was the dominant cavity. Since the diode facet was not AR-coated, the influence of the diode cavity was still visible; it acted as an etalon inside the external cavity and did not allow oscillation when there was destructive interference between the internal and external cavities; thus, for an uncoated laser, the frequency could not be grating-tuned without mode hops.

Our initial attempts to AR-coat two of these lasers were not successful; however, more recent tests by us with a re-coated device (laser 1) show good results, as indicated by a large increase in the feedback sensitivity. The original coating was removed and a new single ($\lambda/4$) layer of SiO ($n \approx 1.9$) was deposited on the InAsSb laser ($n \approx 3.5$). The coating has survived more than 10 temperature cycles to date.

3 Conclusion

In conclusion, we can report that we have developed a cryostat for operation of LN₂-cooled mid-infrared diode lasers, and this cryostat contains the essential optics for external-cavity grating-tuned operation of an uncoated InAsSb laser near $3.4\text{ }\mu\text{m}$. We succeeded in tuning the dominant mode of the diode laser by about 1.44 THz (48 cm^{-1}) through rotation of the in-chamber diffraction grating. In order to achieve reliable single-mode operation and to obtain grating-tuning without mode hops, AR coating of the laser facet was found to be essential. We also used the same setup to investigate the operation of the lead-salt diode lasers for $3\text{ }\mu\text{m}$ in an ECGT configuration. For comparison, it is worth noting that in this case we had some success with our coating efforts (residual reflectance on the order of 1%), but grating control seems just beyond our reach at the moment. We speculate that higher internal photon losses or a more complex spatial mode structure complicate the operation in an ECGT configuration in this case.

Acknowledgements. We are grateful to F. Tittel at Rice University for the chance to test the capability of these novel diode lasers¹. We also thank R. Fox of our group for helpful discussions regarding feedback optics. M.M. acknowledges support from the Deutsche Forschungsgemeinschaft.

References

1. A. Popov, B. Scheumann, R. Mücke, A. Baranov, V. Sherstnev, Y. Yakovlev, P. Werle: *Infrared Phys. Technol.* **37**, 117 (1996)
2. M. Aidaraliev, N.V. Zotova, S.A. Karandashov, B.A. Matveev, N.M. Stus, G.N. Talakin: *Infrared Phys. Technol.* **37**, 83 (1996)
3. A. Popov, V. Sherstnev, Y. Yakovlev, R. Mücke, P. Werle: *Appl. Phys. Lett.* **68**, 2790 (1996)
4. K. Petermann: *Laser Diode Modulation and Noise* (Kluwer Academic, Dordrecht 1988)
5. M. Ohtsu: *Highly Coherent Semiconductor Lasers* (Artech House, Boston 1992)
6. H.Q. Le, G.W. Turner, J.R. Ochoa, M.J. Manfra, C.C. Cook, Y.H. Zhang: *Appl. Phys. Lett.* **69**, 2804 (1996)
7. I.I. Zasavitskii, Y.V. Kosichkin, P.V. Kryukov, A.I. Nadezhdinskii, A.N. Perov, S. Raab, E.V. Stepanov, A.P. Shotov: *Sov. J. Quantum Electron.* **13**, 256 (1983)
8. M. Mürtz, M. Schaefer, M. Schneider, J.S. Wells, W. Urban, U. Schiessl, M. Tacke: *Opt. Commun.* **94**, 551 (1992)
9. M. Mürtz, M. Schaefer, T. George, J.S. Wells, W. Urban: *Appl. Phys. B* **60**, 31 (1995)
10. A. Popov, V. Sherstnev, Y. Yakovlev, R. Mücke, P. Werle: *SPIE Proc.* **2834**, 46 (1996)
11. P. Zorabedian: in *Tunable Lasers Handbook*, ed. by F.J. Duarte (Academic Press, San Diego 1995) pp. 349–442
12. M. Mürtz, J.S. Wells, L. Hollberg, T. Zibrova, N. Mackie: *Toward extended-cavity grating-tuned mid-infrared diode laser operation*, NIST Tech. Note **1388** (1997)

¹For the purpose of clarifying the experimental conditions in our report, we acknowledge that the diode laser manufacturer is the Infrared Optoelectronic Laboratory, IOFFE Physico-Technical Institute, Politechnicheskaya 26, 194021 St. Petersburg, Russia, although the mention of the name of a manufacturing entity does not constitute a NIST endorsement of their products.